The Egyptian Journal of Hospital Medicine (Oct. 2015) Vol. 61, Page 591- 614

Histological and Immunohistochemical Studies on the Kidneys of Pregnant Rats Treated with Clarithromycin

Abdel Razik H. Farrag[a], Gabri MS[b], Asmaa M. Kandil[c], Basma N. Hassan[b], Doaa Ezz-Eldin I. S. [b]

[a] Pathology Department, Medical Research Division National Research Centre, Cairo, Egypt.
[b] Zoology and Entomology Department, Faculty of Science, Helwan University, Cairo, Egypt.
[C] Pharmacology Department, National Organization for Drug Control and Research, Giza, Egypt.

ABSTRACT

Background: clarithromycin is a semisynthetic macrolide antibiotic, exhibits broad-spectrum activity against gram-positive and gram-negative aerobes. Macrolides are bacteriostatic antibiotics that inhibit protein biosynthesis via reversible binding to the bacterial 50S ribosomal subunit. Macrolides are able to cross placenta and reach the fetus.

Aim of the work: the present study is focused on evaluating the effects of antimicrobial drug, clarithromycin on the kidneys of pregnant rats.

Material and methods: clarithromycin is orally given to the treated groups of the pregnant rats once daily at different periods of gestation by gastric tube at a dose of 45 mg/kg/day. The excised kidneys were dissected, processed and stained with H & E, PAS, Masson's trichrome, Feulgen reaction and anti-CD68 immunohistochemical stain then followed by morphometric measurements and statistical analysis. The kidneys were also preserved for DNA fragmentation assay.

Results: this study revealed that clarithromycin administration especially to pregnant rats showed different histopathological and histochemical changes in kidney tissues and cellular DNA. Also immunohistochemical anti-inflammatory marker CD68 showed positive reactivity in all treated groups.

Conclusion: The presence of histopathological and histochemical changes revealed nephrotoxicity in the pregnant rats after administration of the antimicrobial drug, clarithromycin.

Key words: Clarithromycin, Antimicrobial drug, pregnant rats, Kidney

INTRODUCTION

Urinary tract infections are common during pregnancy due to hormonal and anatomo-physiological changes that facilitate the growth and dissemination of bacteria in the maternal urinary tract.[1]

All antibiotics used in human therapy since the dawn of the antibiotics era in the early 1900s can be divided into three distinct categories according to how they were ultimately manufactured on large scale. These categorizations are 'Natural products': compounds manufactured directly by large-scale fermentation of bacteria or fungi 'Semisynthetic antibacterial compounds manufactured by chemical synthesis using a natural product as starting material, and 'Fully synthetic antibacterial compounds that are manufactured by fully synthetic routes [2].

Clarithromycin is a semisynthetic macrolide antibiotic that exhibits broad-spectrum activity against gram-positive and gram-negative aerobes. It is known to have better oral bioavailability and tissue penetration [3]. Clarithromycin acts by binding to the peptidyl transferase region of 23S rRNA and inhibits bacterial protein synthesis. [4]

Clarithromycin is metabolized in the liver via the cytochrome P450 isoenzymes of the CYP3A family. Therefore, drug interactions are an important potential cause of side effects. Adverse effects of this compound in the central nervous system (CNS) include CNS depression (confusion and obtundation) or excitation (agitation, insomnia, delirium and psychosis). Unfortunately, it remains unclear what mechanisms underlies the change in mental status[5].

The antibacterial spectrum of macrolides includes predominantly gram-positive *cocci*, *chlamydia*, *mycoplasma* and *legionella*, *campylobacter coxiella, bartonella*, *corynebacteria* and several *mycobacterium* species. Macrolides are suitable alternatives for patients who are allergic to penicillin [6]

MATERIALS:

1- Drug and dosage:

Clarithromycin $C_{38}H_{69}NO_{13}$, provided by Kahira Pharmaceuticals and Chemicals, Egypt, in a commercial product called Klacid XL in the form of 14 film coated tablets. The tablet was crushed to powder and added to

Received:9/01/2015
Accepted:9/11/2015
DOI : 10.12816/0018763

distilled water. The drug was orally given to the treated group of pregnant rats once daily at different periods of gestation by gastric tube at a dose of 45 mg/kg/day. The dose was equivalent to the therapeutic dose of human (500 mg/day) as calculated according to interspecies dosage conversion scheme of *Paget and Barnes*[7]. The given volume was adjusted so that each 100 g animal body weight received 1ml solution containing the required dose

2- Experimental animals:

The present experimental study was carried out on the adult female and male albino rats (*Rattus norvegicus*); weighing 140–200 grams. The animals were obtained from the National Organization for Drug Control and Research (NODCAR, Cairo, Egypt). Male and female rats were housed separately in metal cages with wire-grid floors. The animals were kept at standard housing facilities (25±2 ºC, 45 ± 5% humidity and 12 hrs. light/dark cycles). They were fed on a standard laboratory chow and water *ad libitum.* The standard guidelines of National Organization for Drug Control and Research (NODCAR) were used in handling animals.

3- Housing and mating:

Adult female rats in proestrus cycle were caged overnight with males of proven fertility. The day on which the sperms were found in the vagina was designated as day zero of gestation (GD) A daily record of the weight of the pregnant females was made. The abortion was determined by the presence of blood drops and sudden drop in the weight of the pregnant females[8].

4- Experimental design:

The pregnant females were randomly divided into six equal groups (n= 6, each) as follow:

Group C1: Pregnant animals received distilled water orally from the day 1 to day 7 of pregnancy. It served as control group, and sacrificed on the 8th day of gestation.

Group T1: Pregnant rats administered clarithromycin orally at a dose of 45 mg/kg/day from the 1st to the 7th day of gestation and sacrificed on the 8th day.

Group C2: Pregnant rats orally administered with distilled water from the 1st to the 7th day of gestation, sacrificed on the 20th day and served as a control group.

Group T2: Pregnant rats orally administered with 45 mg/kg/day of clarithromycin from the 1st to the 7th day of gestation and left to the 19th day and sacrificed on the 20th day.

Group C3: Pregnant animals orally administered with distilled water from the 15th to the 19th day and sacrificed on the 20th day of gestation and served as a control group.

Group T3: Pregnant animals were orally administered with clarithromycin at a dose of 45 mg/kg/day from the 15th to the 19th day and sacrificed on the 20th day .

5- Tissues sampling:

At the end of the experiment, the pregnant animals were sacrificed by decapitation. Kidneys were rapidly excised then, half of each was stored at -80°C for isolation of the genomic DNA and the other half was fixed immediately for histopathological, histochemical, immunohistochemical and histomorphometrical investigations.

METHODS:

1- **Histological and histochemical examination:**

The excised organ was fixed in 10% neutral buffered formalin solution for about 24 hours, washed in running water, dehydrated, cleared in xylene and impregnated in parablast for blocking. Serial sections of 5 µm thick were prepared and stained with: Hematoxylin and Eosin, Periodic acid Schiff's, Masson's trichrome and Feulgen reagents.

2- For immunohistochemical examination:

5 µm sections of kidneys were fixed in 10 % neutral buffered formalin fixative immunostained using anti- CD68 primary antibody (Labvision, Neomarkers, USA) for 90 minutes. This was followed by the secondary antibody application using the immunoperoxidase technique (Vectastain ABC kit; Vector Laboratories, Burlingame, CA).

3- DNA fragmentation assay

DNA fragmentation was determined via agarose gel electrophoresis**;** genomic DNA was isolated from the kidney tissue of the pregnant rats according to **Miller *et al.*** [9] using DNA Purification Kite Promega, Promega Corporation, USA. Agarose gel electrophoresis of DNA was done according to the method of **Sealey and Southern [10].**

4- Morphometric measurements:

Histomorphometric measurements were performed using Leica Qwin 500 Image Analyzer (LEICA Imaging systems Ltd,

Cambridge, London) in Pathology Department, National Research Centre, Cairo. The measurements included the glomerular diameter in H&E stained sections, nuclear area of the convoluted tubular cells in Feulgen stained sections, the basement membrane thickness and the lumen area of the convoluted tubules in sections stained with PAS reaction. The values were measured in fifty random sections per group at magnification X400 The mean grey of carbohydrate content and DNA content, and the mean area percent of collagen in Masson's trichrome stained slides and CD68 +ve immunoreaction were measured within 10 non-overlapping fields/ section for each animal, at X400 magnification.

5- Statistical analysis:

The morphometric results were expressed as mean ± standard errors (SE). Statistical analysis was carried out using the "prism version 5" statistical software. Comparison between different groups was done using one way analysis of variance (ANOVA) followed by Tukey test [11]. The results were considered statistically significant when the (p) value was $P< 0.05$.

RESULTS

I. Histopathological investigations:

I.1. Hematoxylin and Eosin stain:

a. Control Animals:

The histological examination of sections of kidney of the pregnant rats showed the normal architecture of renal corpuscles and tubules (Fig. 1). Renal corpuscles consisted of : a thin walled cup like expansion called the Bowman's capsule and a tuft of capillaries called the glomerulus, which is invaginated into Bowman's capsule, being separated from it by the subscapular space or Bowman's space or urinary space. The outer layer (parietal) of the Bowman's capsules is formed of simple squamous epithelium.

Normal proximal convoluted tubules appears with epithelial lining made up of pyramidal eosinophilic cells with basally located spherical nuclei .The distal convoluted tubules are lined with faint acidophilic cubical cells with spherical nuclei. Their lumens are apparently wider than that of the proximal convoluted tubules (Fig. 1).

b. Treated Animals:

Histopathological examination of kidney of mothers of group T1 showed inflammatory cells in the interstitial tissue and around some of the renal corpuscles (Fig.2). The renal tubular epithelial cells showed different signs of degeneration such as necrosis (Fig. 5), cloudy swelling, vacuolations (Fig. 3), and nuclear pyknosis, karyorrhexis or karyolysis (Fig. 2). Some tubuler detached cells were located in the lumens of their tubules (Fig. 2). Congestion in the glomerular capillaries and the interstitial tissue were shown (Fig.3.4). A complete obliteration of some tubular lumen was seen (Fig. 3). Fibroblasts among the inflammatory cells in the interstitium (Fig. 6) and hemorrhage in interstitial tissue (Fig. 3) were also shown. The capillary tuft of the glomeruli appeared congested, swollen and the Bowman's space is absent (Fig. 4). Lobulation of the glomeruli was seen (Fig. 5).

kidneys of pregnant rats (group T2) produced some pathological changes such as congestion in blood capillaries of the glomerular tufts and hemorrhage in the interstitium (Fig. 7). The convoluted tubules exhibited cloudy swelling with obliterated lumen (Fig. 7). The karryorhetic and karyolytic nuclei and cell detachment were shown in some renal tubules (Fig. 7). Nuclear pyknosis, vacuolations and deeply eosinophilic tubular cells representing necrosis were also seen (Fig. 8). There were mild inflammatory cells in the interstitium and atrophied renal corpuscle (Fig. 8). Some glomeruli exhibited enlargement and congestion with obliterated urinary space (Fig. 9) and the others showed shrunked glomeruli (Fig. 10).

The dams (group T3) displayed cloudy swelling with complete obliteration of the lumens of some renal tubules and their cells showed, vaculation, pyknosis, karryorhexis, karyolysis and Cell detachment (Fig. 11). Congestion and lobulation of the glomerular tuft (Fig. 14), hemorrhage in the interstitium (Fig. 11) and severe infiltration of inflammatory cells in interstitial tissue (Fig. 15) were shown. Capillary tuft of some glomeruli appeared swollen and Bowman's space was narrow (Fig. 12). Also atrophied and completely degenerated glomeruli were seen (Fig. 13).

I.2. Masson's trichrome stain:

a. Kidney cortex of control animals:

Examination of kidneys of control pregnant rats stained with Masson's trichrome showed the appearance of thin collagen fibers stained with a blue color in the cortical tissues including the capsular wall, peritubular and around the blood vessels (Fig. 16).

b. Treated Animals:

Animals of T1 showed a highly increased collagen fibers in tubular interstitium and pericapsular walls (Fig. 17), and also a thick layer of collagen fibers in the interstitium was found in group T1 (Fig. 18) while mild to moderate increase in collagen fibers in tubulointerstitium were shown in group T2 (Fig. 19)

A great increment of collagen fibers around the bowman's capsule wall and peritubules (Fig. 20) were observed in the kidneys of dams of group T3 as compared to the control.

II. Histochemical Results:

II.1. Carbohydrates Content:

a. Kidney cortex of control animals:

Examination of kidneys of control pregnant rats stained with PAS reaction showed the positive materials in the basement membranes of the glomerular capillaries, renal tubules and the brush borders also,exhibited strong positive PAS reaction. (Fig. 21).

b. Treated Animals:

Microscopic observation of kidneys of groups T1 (Fig. 22) showed a a weak PAS reaction in the brush borders of some proximal convoluted tubules (PCTs). There was a thickening in the basement membrane of Bowman's capsule and some renal tubules.

The kidney sections of mother's rats (group T2) (Fig. 23) displayed a weak PAS reaction in the brush borders in few PCTs, also thickness of the basement membranes of some renal tubules was seen.

Examination of sections of kidneys of dams (group T3) (Fig. 24) showed a weak PAS reaction in the brush borders and a thickness of the tubular basement membranes.

2. DNA Content:

Kidney cortex of control animals:

Kidney sections of a control pregnant rats (Fig. 25) shows normal distribution of DNA content. Most of the nuclei are approximately in the same size and strongly stained with magenta color by using Feulgen method.

a. Treated Animals:

DNA content of kidney sections from group T1 and T2, showed that most nuclei were faintly stained magenta color with the appearance of nuclear karyolysis (Fig. 26 and 27, respectively).

Sections from group T3, showed weak staining indicating a marked diminution in DNA of most nuclei of the renal cortex tubules and karyolytic nuclei (Fig. 28).

Immunohistochemical investigations:

III.1. CD68 immunohistochemical detection:

a. Control Animals:

Examination of kidneys of control pregnant rats showing rarely demonstration of CD68-positive macrophages in the tubular interstitium (Fig. 29) and absence of macrophage infiltration in the mesangial areas of the glomeruli (Fig. 30). Negative immunoreactivity for CD68 in the cytoplasm of tubular epithelial cells was found (Fig. 30).

b. Treated Animals:

Kidney sections from group T1 showed a strong to weak CD68-positive reaction in the tubule-interstitium and mesangial areas, respectively (Fig. 31 and 32, respectively). On the other hand, CD68-positive cells were found in some renal tubules (Fig. 32).

Faint CD68-positive reaction in cells of some renal tubules (Fig. 34) and a moderate CD68-positive reaction in the tubulointerstitium (Fig. 33) appeared in the kidney tissues of pregnant rat of group T2 .

Kidney sections of group T3 showed an intensive immunoreactivity for CD68 in the interstitial tissue (Fig. 35) and moderate CD68-positive in some tubules (Fig. 36).

IV. Histomorphometric analyses:

The renal sections of mothers groups stained with Masson's trichrome and anti-CD68 techniques were subjected to image analysis for the determination of mean area percent of collagen contents and CD68 +ve reaction, respectively, and those stained with PAS and Feulgen techniques were subjected to image analysis for determination of the mean grey level of carbohydrate and DNA content, respectively. All data were represented in Table 1 and Figures 37, 38, 39 and 40.

The kidney sections of mothers of (group T1) showed significant increase in the

mean area % of collagen contents and CD68 +ve Rx, and the mean grey of carbohydrate and DNA content at $P<0.05$ as compared to control group (group C1) recording 115.23, 848.02, 7.86 and 7.16, respectively as a percentage difference.

The sections of kidneys of mothers (group T2) showed non-significant changes in the mean area % of collagen contents and in the mean grey of carbohydrate content at $P<0.05$ as compared to the control group, while the mean area % of CD68 +ve Rx and the mean grey of DNA content showing a significant increase as compared to the control group (group C2) at $P<0.05$ reading 477.8 and 5.72 as a percentage difference.

The kidney sections of mothers of group T3 showed histochemical changes as indicated by the significant increase at $P<0.05$ in the mean area % of collagen contents and CD68 +ve reaction, and the mean grey of carbohydrate and DNA content as compared to control group (group C3) (91, 581.3, 9.21and 9.55, respectively).

The kidney sections of dams groups were subjected to histomorphometrical measurements of the glomerular diameter, and the convoluted tubules- (CT) nuclear area, lumen area and basement membrane (BM) thickness. These data were represented in Table 2 and Figs. 41, 42, 43 and 44.

Data obtained from histomorphometrical measurements of kidneys of (group T1) demonstrated non-significant changes in the mean values of CT BM thickness and a significant increase ($P<0.05$) of the mean values of the glomerular diameter in comparison with control group (group C1) recording 11.74. On the other hand, there was a significant decrease at $P<0.05$ in mean values of CT nuclear area and lumen area as compared to the control group value (-17.92 and --29.70, respectively).

Non-significant changes were shown in the mean values of glomerular diameter and CT BM thickness of mothers (group T2) as compared to the control group ($P<0.05$), whereas the mean values of nuclear area and lumen area of CT showed significant decrease at $P<0.05$ when compared to control group (group C2) (-14 and -22.22, respectively).

The mean value of CT BM thickness was non-significantly changes and the mean values of glomerular diameter was significantly increased ($P<0.05$) reading 9.13 as percentage differences in kidneys of mothers of (group T3) as compared to the control group, while a significant decrease ($P<0.05$) in the mean values of nuclear area and lumen area of CT and these values were -18 and -26.34, respectively as compared with untreated group (group C3).

V. Molecular investigations:

V.1. <u>Determination of DNA purity</u>:

The total genomic DNA isolated from kidney of pregnant rats was evaluated for purity and the results were summarized in Table (3) and they nearly showed the absence of contamination in all samples.

V.II- <u>Agarose gel electrophoresis of DNA:</u>

Agarose gel electrophoresis of DNA was done for determination of total genomic DNA Fragmentation. As shown in Figure (45), the DNA from renal cells of control pregnant rats (group c) was found to be intact (undamaged) as seen in lane 2, while the DNA from others groups showed a degree of DNA damage of smear pattern which indicates the presence of necrosis.

Severe to moderate DNA smear formation was shown in lane 3 and 4, respectively of the group T1 and T2 indicated an intense to moderate damage in DNA of renal cells.

The DNA from group T3 showed strong DNA damage of smear pattern in lane 5 which indicates to the presence of necrosis.

DISCUSSION

In the present study, the histopathological examination showed that the oral administration of therapeutic dose (45 mg/kg/day) of as clarithromycin at different periods during pregnancy in rats induced nephrotoxicity

The kidney plays an important role in the elimination of numerous hydrophilic xenobiotics, including drugs, toxins, and endogenous compounds[12], [13]. Clarithromycin was reported to obtain higher concentrations than erythromycin in the kidney [17]. 30% to

40% of an oral dose of clarithromycin is excreted in the urine via glomerular filtration of the kidney[18].

During pregnancy, the sensitivity for toxic compounds is increased [19]. Pregnancy has been reported to alter the expression and activity of drug metabolizing enzymes significantly; and these changes are likely to

have toxicological and therapeutic implications[20].

A significant potential of clarithromycin to cause nephrotoxicity in man was reprted by *Chapelsky et al* [14] aftrer administration of 13 therapeutic doses of the drug (500 mg orally) every 12h. However, low potential for clarithromycin nephrotoxicity in rats, dogs and primates have been reported by *Guay et al.* [15].

The nephrotoxicity of clarithromycin might happen due to the induction of oxidative stress in the renal tissue. *Olayinka and Ore* [16] found that oral administration of clarithromycin has adverse effects on both enzymic and non-enzymic antioxidant status and induces oxidative stress,

Oxidative stress is a common pathogenic mechanism contributing to initiation and progression of cell damage [24]. The oxidative stress refers to a cell's state characterized by excessive production of reactive oxygen species (ROS) and/or reactive nitrogen species (RNS) and/or a reduction in antioxidant defenses responsible for their metabolism [25], [26].

Damage induced by ROS includes alterations of cellular macromolecules such as membrane lipid, DNA, and/or protein. The damage may alter cell function through changes in intracellular calcium or intracellular pH, and eventually can lead to cell death [27], [28].

Most drugs that to cause nephrotoxicity were reported to exert toxic effects by one or more common pathogenic mechanisms. These include altered intraglomerular hemodynamics, tubular cell toxicity, inflammation, crystal nephropathy, rhabdomyolysis, and thrombotic microangiopathy [29]. In the present study, nephrotoxicity by clarithromycin (45 mg/kg) on the pregnant rats at different periods of gestation was judged by the histopathological changes including congestion, lobulation and enlargement of capillary tuft of the glomeruli leading to the absence of the urinary space. Partial degeneration with shrinkage of glomeruli leading to dilatation in Bowman's space or completely degeneration of glomeruli or atrophied corpuscles also appeared. Hydropic degeneration, nuclear pyknosis, karyorrhexis, karyolysis, vacuolations and deeply eosinophilic cells representing necrotic cells in the epithelium lining the renal tubules were also seen. The renal tubules showed cloudy swelling in their cells leading to the appearance of small or completely obstructed lumen. Also the detached cells of some renal tubular epithelial cells appeared in the lumen. Hemorrhage, inflammatory cells infiltration and fibrosis were detected in the interstitium.

Renal tubular cells, in particular proximal tubule cells, are vulnerable to the toxic effects of drugs because their role in concentrating and reabsorbing glomerular filtrate exposes them to high levels of circulating toxins[30]. Drugs that cause tubular cell toxicity do so by impairing mitochondrial function, interfering with tubular transport, increasing oxidative stress, or forming free radicals [31].

A significant increase in the mean value of glomerular diameter of the kidneys of the treated pregnant rats at $P<0.05$ in comparison with the control group was recorded in the present study. Also, clarithromycin treatment induced inflammatory infiltration in the interstitium and these results disagree with those of *Özdemir et al.* [32] who stated that clarithromycin had a protective effect on bowel injury owing to anti-inflammatory effects. Tubulointerstitial inflammation may result from leakage of filtered urine to the interstitial space through capsular adhesions[33]. The works of *Kriz and LeHir* [34] have exquisitely shown the formation of bridges between podocytes and the Bowman's capsule in sites of capsular adhesions and a remaining narrow urinary space allows leakage of ultrafiltrate to tubulointerstitial areas. According to *Cotran et al.* [35] inflammation is fundamentally a protective response whose ultimate goal is to rid the organism of both the initial cause of cell injury and the consequences of such injury, the necrotic cells and tissues. Inflammation serves destroy, dilute, or wall off the injury agent. In this study, the mean values of lumen area of the convoluted tubules of the kidneys of the treated pregnant rats showed a significant decrease ($P<0.05$) in comparison with the control group. This result appeared in H&E stained sections as cloudy swelling in the epithelial cells of convoluted tubules with partial or complete obstruction of their lumen. The morphology of necrosis is characterized by swelling and degeneration of the entire cytoplasm[36]. *de Wardener* [37] described the cloudy swelling mechanism and stated that many disease processes may directly inhibit the sodium pump of the cell. Sodium then accumulates within

the cell and subsequently by water is drown into the cell causing cloudy swelling [38].

Vacuolations and deeply eosinophilic cells in the epithelium lining the renal tubules were seen in this work. Vacuolation and deeply eosinophilic cells, representing degenerating cells, in the epithelium lining the proximal renal tubules [39], [40]. Degeneration may occur as a direct adverse effect of a metabolite or xenobiotic on the tubules[41]. Degeneration may started with swelling of the cell and mitochondrial contents, followed by rupture of the cell membrane[42]. Necrosis can trigger an inflammatory reaction in the surrounding tissue as a result of the release of cytoplasmic contents, many of which are proteolytic enzymes [43].

Hemorrhage in the interstitium was shown in the present study in the kidneys of the treated pregnant rats . This result agrees with those of ***Olayinka and Ore*** **[44]** who reported that foci of haemorrhages in the renal cortex were observed after administration of the 17.6 mg kg-1 clarithromycin. Hemorrhage often accompanies acute injury and can occur in the kidney as a primary lesion associated with nephrotoxicants. Hemorrhage can occur from inflammation, tubular necrosis, and vascular injury or from the presence of calculi or tumors[45].

Examination of kidneys of control pregnant rats showed rarely demonstration of CD68-positive macrophages in the tubular interstitium and absence of macrophage infiltration in the mesangial areas of the glomeruli. Negative immunoreactivity for CD68 in the cytoplasm of tubular epithelial cells was found. While, the kidneys sections from of the treated groups of pregnant rats examined after treatment with clarithromycin (45 mg/kg) showed a CD68-positive cells in the tubulointerstitium indicating the presence of the macrophage infiltration. Also, CD68-positive reaction was found in mesangial areas and the cytoplasm of some tubular cells. So, there is a significant increase in the mean area % of CD68 +ve Rx at P< 0.05 of the kidneys of the treated pregnant rats as compared to control group.

CD68 is related to the family of lysosomal associated proteins [46], and expressed in cytoplasm and on the cell surface [47]. In general, this antigen is expressed by the majority of tissue macrophages and increase surface expression in mature macrophage. Tubular epithelial cells have the potential to transdifferentiate into CD68 positive macrophage-like cells in association with oxdative stress [48]. *Oda et al.* [49] termed intratubular CD68-positive cells "giant macrophages". *Bariety et al.* [50], [51] suggested that podocytes undergo a process of transdifferentiation and acquire macrophage epitopes. In Masson's trichrome stain, sections of the kidneys of the treated pregnant rats showed an increased collagen fibers in the glomeruli accompanied by areas of tubulointerstitial fibrosis and around the Bowman's capsules. So, there is a significant increase at P< 0.05 in the mean area % of collagen contents in the kidneys of the treated pregnant rats as compared to control group.

In the present work clarithromycin treatment induced inflammatory infiltration in the interstitium. *Perazella* [33] stated that drugs can cause inflammatory changes in the interstitium, leading to fibrosis.

During renal disease, the infiltration of monocytes/macrophages and T cells into kidneys is thought to play a central role in progressive interstitial fibrosis and the progression of renal failure [52].

Tubulointerstitial fibrosis is a common feature of progressive renal injury in almost all forms of renal diseases **[53]**. It has been shown that tubulointerstitial injury is a more consistent predictor of functional impairment than glomerular damage [54]. Chronic inflammation generally precedes the development of fibrosis and inflammatory cytokines are important mediators of fibrogenesis [55].

The cortical interstitium is normally composed of a network of fibroblasts and dendritic cells with only a small number of lymphocytes or macrophages [56]. In chronic interstitial fibrosis, the interstitial cells have myofibroblast characteristics which are considered to be derived from the proliferation and differentiation of the residual fibroblasts [57].

In the present study clarithromycin treatment induced glomerular atrophy. Glomerular atrophy is a sequel to chronic degenerative changes in the glomeruli and subsequent hemodynamic alterations [58]. It is characterized by shrinkage and contraction of the capillary tufts, often with a corresponding dilation of Bowman's space [45]. Once hemodynamic or degenerative changes in the

glomerulus are initiated, a complex sequence of events within the mesangium and podocytes are initiated, mediated by TGF-beta and CTGF, which result in the stimulation of fibroblast proliferation and collagen formation with the eventual replacement of normal architecture [34], [59].

Oxygen and nitrogen free radicals are highly reactive and are capable of damaging macromolecules like carbohydrates **[60]**. So, there was decrement of polysaccharides contents in tubular cells of the kidneys of the treated pregnant rats. Also, there were destruction and thinning of brush border of the proximal tubules. *Lameire and Vanholder* [61] had reported that loss of the brush border was appeared in kidneys suffering from toxicological insult. A significant increase of the mean grey of carbohydrate content at $P< 0.05$ was shown in renal sections of pregnant rat treated with 45 mg/kg clarithromycin orally as compared to control which confirmed the decrement of polysaccharides content.

In this study, necrosis was assessed in the kidneys of the treated pregnant rats stained with H&E stain and/or Feulgen technique with the appearance of pyknosis, karyorrhexis or karyolysis (very weak stain with F). These results were confirmed with measuring the mean values of nuclear area of the convoluted tubules that showed a significant decrease ($P<0.05$) in comparison with the control group. Also, the karyolysis was indicated by the significant increase at $P<0.05$ in the mean grey of DNA content as compared to control group. The genomic DNA from renal cells of the pregnant rats after the treatment of 45 mg/kg of clarithromycin and their yielded fetuses showed a degree of DNA damage of smear pattern which indicates to the presence of necrosis. The degradation of DNA may be due to the increased ROS **[62]** and RNS (e.g. Peroxynitrite) which interact with cellular macromolecules such as DNA and causes chemical cleavage of DNA **[63]**.

Pyknosis, or shrunken nuclei, is the irreversible condensation of chromatin in the nucleus of a cell undergoing necrosis **[64], [65]** or apoptosis **[66]**. It is followed by karyorrhexis which is the destructive fragmentation of the nucleus of a dying cell **[67]** involving loss of integrity of the nucleus. Karyolysis is the complete dissolution of the chromatin of a dying cell due to the enzymatic degradation by endonucleases. The whole cell will eventually stain uniformly with eosin after karyolysis in which a Feulgen-negative, ghost-like image of the nuclei remained**[64]**. It is usually preceded by karyorrhexis and occurs mainly as a result of necrosis, while in apoptosis after karyorrhexis the nucleus usually dissolves into apoptotic bodies [67], [68].

Finally, the above-stated findings lead to the conclusion that the presence of the histopathological changes revealed nephrotoxicity in the pregnant rats after administration with 45 mg/kg once daily of the antimicrobial agent, clarithromycin, which equal to the therapeutic dose of human 500 mg of clarithromycin extended release tablets once daily. So, clarithromycin is not safe for pregnant rats and it should not be used except under strict conditions in medication.

REFERENCES

1- Souzaa B R, Trevisol J D and Trevisol S F **(**2015**)**: Bacterial sensitivity to fosfomycin in pregnant women with urinary infection. j. Infect. Diseases, 9(3): 319–323.

2- Wright P M, Seiple I B and Myers A G (2014): The Evolving Role of Chemical Synthesis in Antibacterial Drug Discovery. Angew. Chem. Int. Ed., 53 (34): 8840 – 8869.

3- Kwak H M, Shin M Y, Cha S J, Choi J H, Lee J S,Kim C R, Roh J H and Kim S y (2013): The efficacy of cefazolin plus macrolide (erythromycin or clarithromycin) versus cefazolin alone in neonatal morbidity and placental inflammation for women with preterm premature rupture of membranes. J. Placenta, 34: 346-352.

4- Melake A N, Shaker H G and Salama A M (2012): Incidence of Helicobacter pylori infection and their clarithromycin-resistant strains in otitis media with effusion regarding phenotypic and genotypic studies. J. Saudi Pharm., 20(4): 345–353.

5- Friese K and Melchert F (2002): Arzneimitteltherapie in der Frauenheilkunde. Wissenschaftliche Verlagsgesellschaft mbH, Stuttgart.

6- Friese K, Mörike K, Neumann G and Windorfer A. (2009) Arzneimittel in der Schwangerschaft und Stillzeit: Ein Leitfaden für Ärzte und Apotheker Wissenschaftliche Verlagsgesellschaft mbH, Stuttgart.

7- Paget G E and Barnes J M (1964): Evaluation of drug activities. "Pharmacometrics." 1st ed. Laurence, Acad. Press, London, N. Y., p. 135.

8- McClain R M and Becker B A (1975): Teratogenicity, foetal toxicity and placental transfer of lead nitrate in rats. Toxicol. Appl. Pharmacol., 31(1): 72-82.

9- Miller S A, Dykes D D and Polesky H F (1988): A simple salting out procedure for extracting DNA from human nucleated cells. Nucleic Acids Res., 16(3): 1215.

10- Sealey P G and Southern E M (1982): Gel Electrophoresis of DNA. In, Gel electrophoresis of nucleic acids; a practical approach (Rickwood D, Hames BD Editors), IRL Press.

11- Armitage P and Berry G (1987): Comparison of several groups. In: Blackwell Scientific Publications, Oxford; 186-213.

12- Launay-Vacher V, Izzedine H, Karie S, Hulot J S, Baumelou A and Deray G (2006): Renal tubular drug transporters. Nephron Physiol., 103: 97–106.

13- Perazella M A (2009): Renal vulnerability to drug toxicity. Clin. J. Am. Soc. Nephrol., 4: 1275–1283.

14-Chapelsky M C, Nix D E, Cavanaugh J C, Wilton J H, Norman A and Schentag J J (1992): Renal tubular enzyme effects of clarithromycin in comparison with gentamicin and placebo in volunteers. Drug Saf., 7(4): 304-309.

15-Guay D R, Patterson D R, Seipman N and Craft J C (1993): Overview of the tolerability profile osaswaf clarithromycin in preclinical and clinical trials. Drug Saf., 8(5): 350-364.

16- Olayinka E T and Ore A (2012): Administration of clarithromycin (claricin ®) induces changes in antioxidant status and biochemical indices in rats. Res. J. Pharmacol., 6 (4): 52-61.

17- Schlossberg D (1995): Azithromycin and clarithromycin. Med. Clin. North. Am., 79: 803–815.

18- Hardy D J, Guay D R and Jones R N (1992): Clarithromycin, a unique macrolide: a pharmacokinetic, microbiological, and clinical overview. Diagn. Microbiol. Infect. Dis., 15: 39–53.

19- Roberts J S and Silbergeld E K (1995): Pregnancy, lactation, and menopause: How physiology and gender affect the toxicity of chemicals. Mount Sinai J. Med., 62: 343–355.

20- Dickmann L J, Tay S, Senn, T D, Zhang H, Visone A, Unadkat J D, Hebert M F and Isoherranen N (2008): Changes in maternal liver Cyp2c and Cyp2d expression and activity during rat pregnancy. Biochem. pharmacol., 7: 1677– 1687.

21- Tulkens P M (1991): Intracellular distribution and activity of antibiotics. Eur., J. Clin. Microbiol. Infect. Dis. 10: 100–106.

22- Carlier M B, Garcia-Luque I, Montenez J P, Tulkens P M and Piret J (1994): Accumulation, release and subcellular localization of azithromycin in phagocytic and non-phagocytic cells in culture., Int. J. Tissue React. 16: 211–220.

23- Foulds G, Shepard R M and Johnson R B (1990): The pharmacokinetics of azithromycin in human serum and tissues. J. Antimicrob. Chemother., 25(A): 73–82.

24- Medina J and Moreno-Otero R (2005): Pathophysiological basis for antioxidant therapy in chronic liver disease. Drugs, 65(17): 2445-2461.

25- Aly N, EL-Gendy K, Mahmoud F and El-Sebae A K (2010): Protective effect of vitamin C against chlorpyrifos oxidative stress in male mice. Pestic. Biochem. Physiol., 97: 7–12.

26- El-Neweshy M S and El-Sayed Y S (2011): Influence of vitamin C supplementation on lead-induced histopathological alterations in male rats. Exp. Toxicol. Pathol., 63: 221-227.

27- Oboh G and Ogunruku O O (2010): Cyclophosphamide induced oxidative stress in brain: Protective effect of hot short pepper (*Capsicum frutescens* L. var. *abbreviatum*). Exp. Toxicol. Pathol., 62: 227– 233.

28- Ryan M J, Dudash H J, Docherty M, Geronilla K B, Baker B A, Haff G G, Cutlip R G and Always S E (2010): Vitamin E and C supplementation reduces oxidative stress, improves antioxidant enzymes and positive muscle work in chronically loaded muscles of aged rats. Exp. Gerontol., 45: 882–895.

29- Schetz M, Dasta J, Goldstein S and Golper T (2005): Drug-induced acute kidney injury. Curr. Opin. Crit. Care, 11(6): 555–565.

30- Perazella M A (2005): Drug-induced nephropathy: an update. Expert. Opin. Drug Saf., 4(4): 689–706.

31- Markowitz G S and Perazella M A (2005): Drug-induced renal failure: a focus on tubulointerstitial disease. Clin. Chim. Acta., 351: 31–47.

32-Özdemir Ö M, Ergin H, Yenisey Ç, Türk N Ş and Şimşek N G (2010): Protective effects of clarithromycin in rats with hypoxia/reoxygenation-induced intestinal injury. J. Pediatr. Surg., 45(11): 2169-2174.

33- Rodríguez-Iturbe B and García G G (2010): The Role of Tubulointerstitial inflammation in the progression of chronic renal failure. Nephro. Clin. Pract., 116: 81–88.

34- Kriz W and Le Hir M (2005): Pathways to nephron loss starting from glomerular diseases: insights from animal models. Kidney Int., 67: 404–419.

35- Cotran R S, Kumar V and Robbins S L (1994): Inflammation and Repair. In: Robbins Pathologic Basis of Disease. 5th ed. Philadelphia, WB Saunders Company, Pp. 51–93.

36- Padanilam B J (2003): Cell death induced by acute renal injury: a perspective on the contributions of apoptosis and necrosis. Am. J. Physiol. Renal Physiol., 284: 608–627.

37- de Wardener H E (1974): The kidney. 4th ed., Chapter 14, Pristol, The English language Book and Churchil livingstone, Pp. 159-170.

38- Manley G T, Binder D K, Papadopoulos M C and Verkman A S (2004): New insights into water transport and edema in the central nervous system from phenotype analysis of aquaporin-4 null mice. Neuroscience, 129: 981–989.

39- Alpers C E (2005): The Kidney. Robbins and Cotran Pathologic Basis of Disease. Edited by

Kumar V, Abbas AK, Fausto N, Philadelphia, Elsevier Inc., 7th ed., Pp: 993-996.

40- Peres L C, Sethuraman C, Al-Adnani M and Cohen M C (2012): Original Article Necrotic epithelial cells in proximal renal tubules of 2nd trimester fetuses: is this "acute tubular necrosis"?. Int. J. Clin. Exp. Pathol., 5(4): 326-330.

41- Harriman J F and Schnellmann R G (2005): Mechanisms of renal cell death. In Toxicology of the Kidney (J. B. Tarloff and J. H. Lash, eds.), 3rd ed., CRC Press, Boca Raton. Pp. 245–297.

42- Majno G and Joris I (1995): Apoptosis, oncosis and necrosis. An overview of cell death. Am. J. Pathol., 146(1): 3-16.

43- Vermes I and Haanan C (1994): Apoptosis and programmed cell death in health and disease. Adv. Clin. Chem., 31: 177-246.

44- Olayinka E T and Ore A (2012): Administration of clarithromycin (Claricin ®) Induces Changes in Antioxidant Status and Biochemical Indices in Rats. Res. J. Pharmacol., 6 (4): 52-61.

45- Seely J, Frazier K S, Hard G C, Betton G, Burnett R, Nakatsuji S, Nishikawa A, Durchfeld-Meyer B and Bube A (2012): Proliferative and nonproliferative lesions of the rat and mouse urinary system. Toxicol. Pathol., 40: 14-86.

46- Fukuda M (1991): Lysosomal membrane glycoproteins. Structure, biosynthesis and intracellular trafficking. J. Biol. Chem., 266: 21327–21330.

47- Ramprasad M P, Terpstra V, Kondratenko N and *et al.* (1996): Cell surface expression of mouse macrosialin and human CD68 and their role as macrophage receptors for oxidized low density lipoprotein. Proc. Natl. Acad. Sci. U. S. A., 93: 14833–14838.

48- Tanaka M, Suzuki Y, Shirato I, Takahara H, Shibata T, Sugaya T, Shimamoto K, Horikoshi S and Tomino Y (2008): Tubular epithelial cells have the capacity to transdifferentiate into CD68-positive macrophage-like cells by oxidative stress. Inflamm. Res. 57: 593–600

49- Oda T, Hotta O, Taguma Y, Kitamura H. and *et al.* (1998): Clinicopathological significance of intratubular giant macrophages in progressive glomerulonephritis. Kidney Int., 53: 1190–1200.

50- Bariety J, Bruneval P, Hill G and *et al.* (2001): Posttransplantation relapse of FSGS is characterized by glomerular epithelial cell transdifferentiation. J. Am. Soc. Nephrol., 12: 261–274.

51- Bariety J, Bruneval P, Hill G S and *et al.* (2003): Transdifferentiation of epithelial glomerular cells. J. Am. Soc. Nephrol., 14: 42–47.

52- Norman J T and Fine L G (1999): Progressive renal disease: Fibroblasts, extracellular matrix, and integrins. Exp. Nephrol., 7:167–177.

53- Cameron J S (1992): Tubular and interstitial factors in the progression of glomerulonephritis. Pediatr Nephrol., 6: 292–303.

54- Tawakal N, Tawakal N and Tahir M (2012): Cyclosporin an induced tubulointerstitial changes in developing kidney. Pak. J. Med. Health Sci., 6(1): 124-128.

55- Strutz F (1995): Novel aspects of renal fibrogenesis. Nephrol. Dial. Transplant, 10: 1526–1532.

56- Kaissling B and Le Hir M (2008): The renal cortical interstitium: Morphological and functional aspects. Histochem. Cell Biol., 130: 247–262.

57- Yang J and Liu Y (2001): Dissection of key events in tubular epithelial to myofibroblast transition and its implications in renal interstitial fibrosis. Am. J. Pathol., 159: 1465–1475.

58- Menini S, Iacobini C, Oddi G, Ricci C, Simonelli P, Fallucca S, Grattarola M, Pugliese F, Pesce C and Pugliese G (2007): Increased glomerular cell (podocyte) apoptosis in rats with streptozotocin-induced diabetes mellitus: Role in the development of diabetic glomerular disease. Diabetologia, 50: 2591–2599.

59- Lee H S and Song C Y (2009): Differential role of mesangial cells and podocytes in TGF-beta-induced mesangial matrix synthesis in chronic glomerular disease. Histol. Histopathol., 24: 901–908.

60- Wang C Y, Mayo M W, Baldwin A S (1996): TNF- and cancer therapy-induced apoptosis: potentiation by inhibition of NF-κB. Science, 274: 784–787.

61- Lameire N and Vanholder R (2000): Pathophysiologic features and prevention of human and experimental acute tubular necrosis. J. Am. Soc. Nephrol., 12(17): 20-23.

62- Song B J, Suh S K and Moon K H (2010): A simple method to systematically study oxidatively modified proteins in biological samples and its applications. Methods Enzymol., 473: 251-64.

63- Chirino Y I, Hernandez-Pando R and Pedraza-Chaverri J (2004): Peroxynitrite decomposition catalyst ameliorates renal damage and protein nitration in cisplatin-induced nephrotoxicity in rats. BMC Pharmacol., 4: 20-29.

64- Jen M H, Hwang J, Yang J, Nabyvanets Y, Hsieh W A, Tsai M, Guo S and Chang W P (2002): Micronuclei and nuclear anomalies in urinary exfoliated cells of subjects in radionuclide-contaminated regions. Mutation Research, 520: 39-46.

65- Kumar V, Abbas A, Nelson F and Mitchell R (2007): "Robbins Basic Pathology". 8th ed., Saunders Elsevier. Pp. 9–10.

66- Kroemer G, Galluzzi L and Vandenabeele P and *et al.* (2009): Classification of cell death: recommendations of the Nomenclature Committee on Cell Death. Cell Death Differ., 16 (1): 3–11.

67- Cotran R, Kumar V and Collins T (1999): Robbins Pathologic Basis of Disease. 6th ed., Philadelphia: W.B. Saunders company. Pp. 7216-7335.

68- Cachat F, Lange-Sperandio B, Chang A Y, Kiley S C, Thornhill B A, Forbes M S and Chevalier R L (2003): Ureteral obstruction in neonatal mice elicits segment-specific tubular cell responses leading to nephron loss. Kidney International, 63: 564-575.

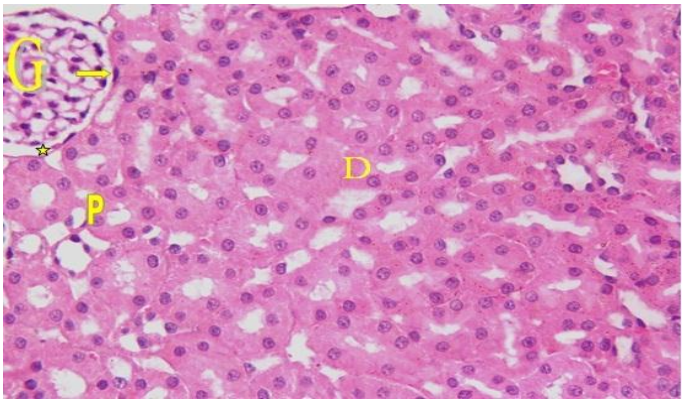

Fig. 1: Photomicrograph of a section of renal cortex of control pregnant rat showing renal corpuscles consisting of glomeruli (G), urinary space (asterisk) and Bowman's capsule (arrow). The distal (D) and proximal (P) convoluted tubules are also well shown. (H&E, x400)

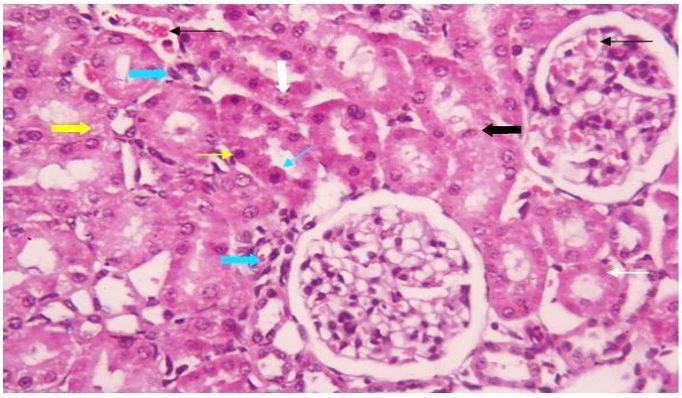

Fig. 2: Photomicrograph of the kidney section of grT1 showing inflammatory cells (blue thick arrow) in interstitial tissue and around renal corpuscle. The renal tubular epithelial cells show cloudy swelling**(blue thin arrow),** vacuolations **(yellow thick arrow),** pyknosis (**yellow thin arrow),** Karyorrhexis **(white thick arrow)** and karyolysis (**white thin arrow).** Some of detached cells present into the lumen tubules **(black thick arrow).** congestion **(black thin arrow)** of the glomerular capillary and the interstitial tissue are shown. (H&E, x400)

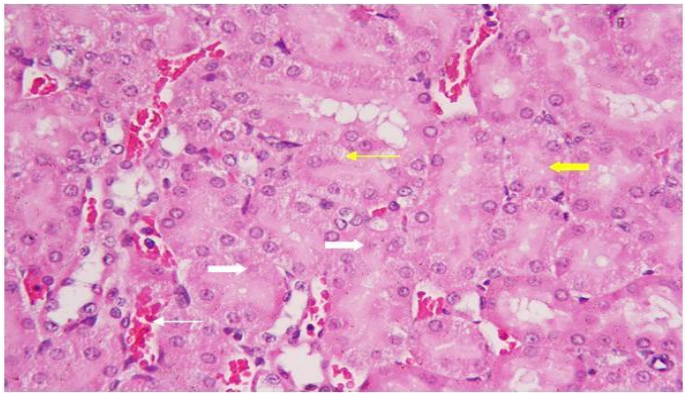

Fig. **3:** Photomicrograph of the kidney section of pregnant rat of gr.T1 showing complete obliteration of the renal tubular lumen is seen **(yellow thick arrow)**. The tubuler cells are extensively vacuolated **(yellow thin arrow)** with many karyolytic nuclei **(white thick arrow)**. Hemorrhage in interstitial tissue (**white thin arrow)** is also seen. (H&E, x400)

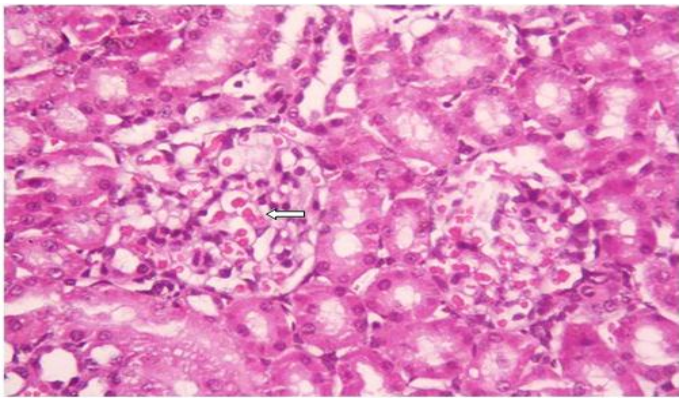

Fig. **4:** Photomicrograph of the kidney section of group pregnant rat of gr.T1 showing congestion and swollen of the capillary tuft of the glomeruli (white thick arrow). (H&E, x400)

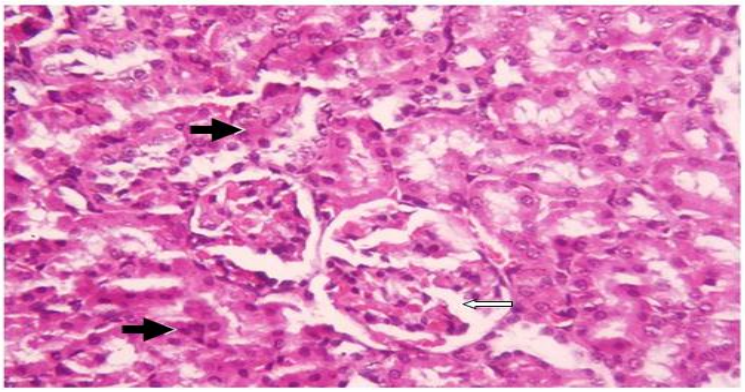

Fig. **5:** Photomicrograph of the kidney section of pregnant rat of gr.T1 showing lobulation of the glomeruli (white arrow) and necrotic tubules (black arrow). (H&E, x400)

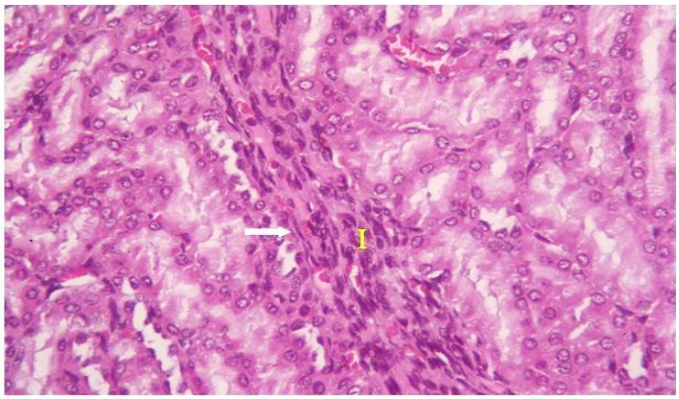

Fig. **6:** Photomicrograph of the kidney section of pregnant rat of gr.T1 showing fibroblasts (arrow) among the inflammatory cells in the interstitium (I). (H&E, x400)

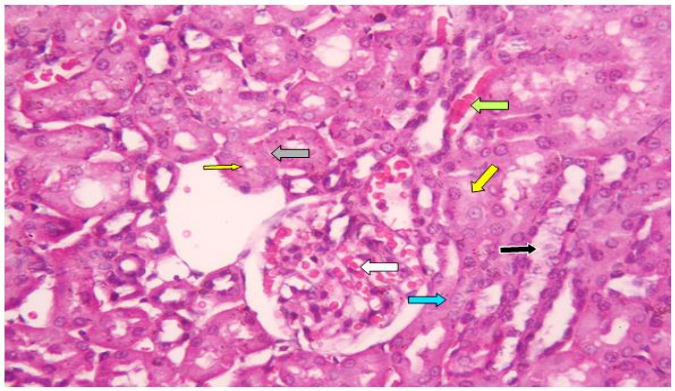

Fig. 7: Photomicrograph of a section of the kidney of pregnant rat of gr.T2 showing congested blood capillaries **(white arrow)** of the glomerular tufts and hemorrhage in the interstitial space **(green arrow).** Cloudy swelling tubular cells with narrow **(yellow thin arrow)** or obliterated **(yellow thick arrow)** tubular lumen are seen Some nuclei of tubular cells showing karryorhexis **(blue arrow)**, karyolysis **(grey arrow)** and detachment **(black arrow). (H&E, x400)**

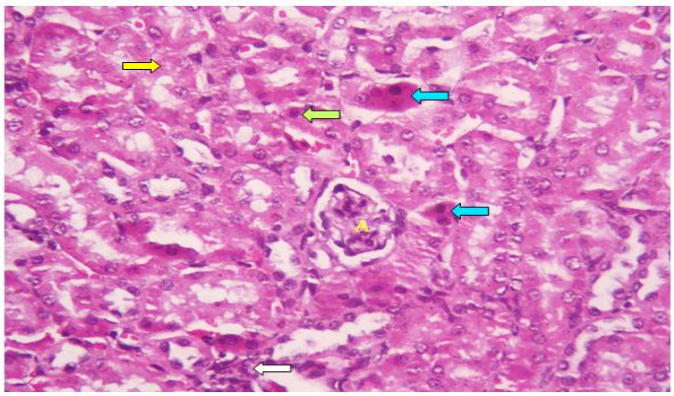

Fig. 8: Photomicrograph of a section of the kidney of pregnant rat of gr.T2 showing atrophied renal corpuscle (A) and mild inflammatory cells in the interstitium **(white arrow).**Nuclear pyknosis **(green arrow),** vacuolations **(yellow arrow)** and necrotic tubuler cells **(blue arrow) (H&E, x400)**

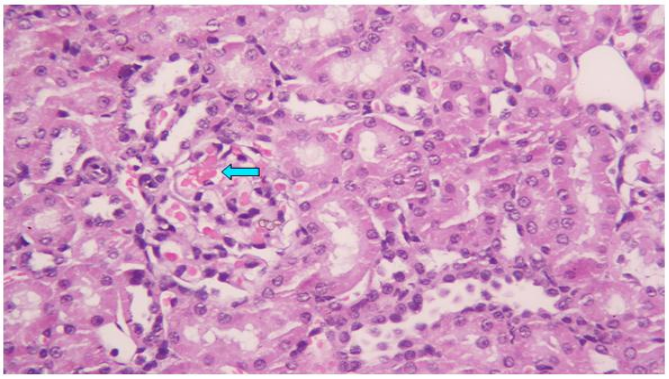

Fig. 9: Photomicrograph of a section of the kidney of pregnant rat of gr.T2 showing enlargement and congestion of the glomerulus (blue arrow) and obliterated urinary space.(H&E,x400

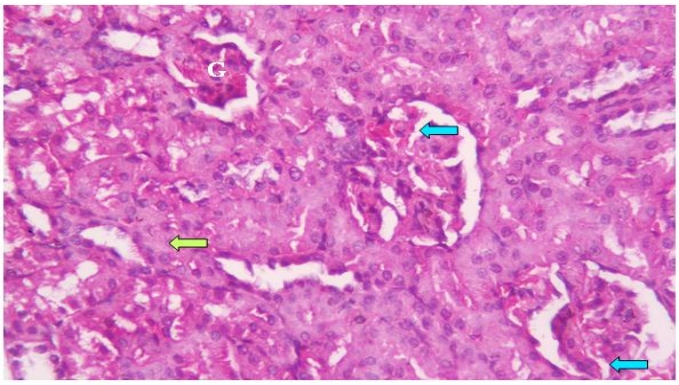

Fig. 10: Photomicrograph of a section of the kidney of pregnant rat of gr.T2 showing a necrotic and shrunken glomerulus (G), and also lobulated glomeruli (blue arrow). The most of tubular lumens are completely obliterated (green arrow). (H&E, x400)

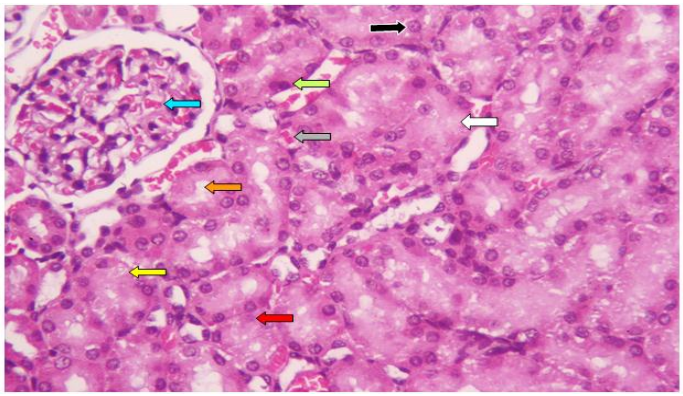

Fig. 11: Photomicrograph of the kidney section of pregnant rat of gr.T3 showing almost complete obliteration of the tubular lumen **(white arrow)** and their cells showing cloudy swelling **(orange arrow),** vaculation **(yellow arrow),** pyknosis **(green arrow),** karryorhexis **(black arrow)** and karyolysis **(red arrow).** Congestion of glomerular tuft **(blue arrow)** and hemorrhage in the interstitium **(grey arrow)** are also shown(H&E, x400).

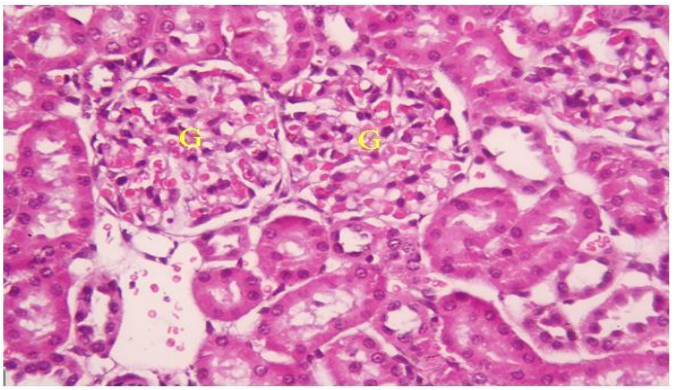

Fig. 12: Photomicrograph of the kidney section of pregnant rat of gr.T3 showing congested and swollen capillary tuft of the glomeruli (G) and the normal space between the capillary tuft and Bowman's capsule is absent. (H&E, x400)

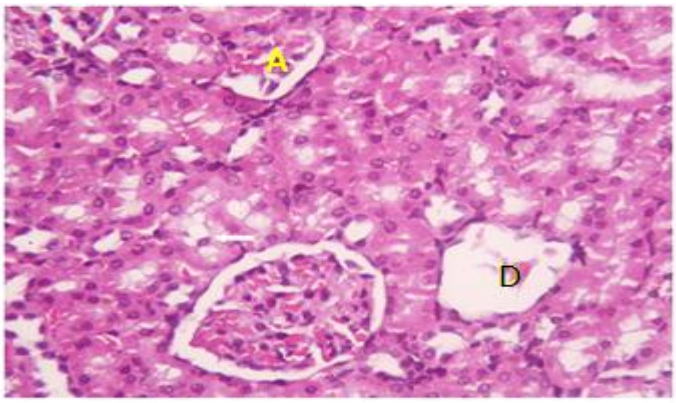

Fig. 13: Photomicrograph of the kidney section of pregnant rat of gr.T3 shows atrophied renal corpuscle (A) and completely degenerated glomeruli (D). Cell detachment (white thick arrow) is shown. (H&E, x400)

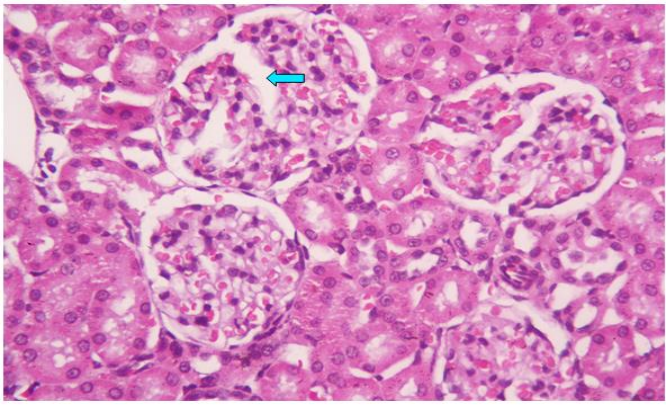

Fig. 14: Photomicrograph of the kidney section of pregnant rat of gr.T3 showing enlarged and lobulated glomeruli (blue thick arrow). (H&E, x400)

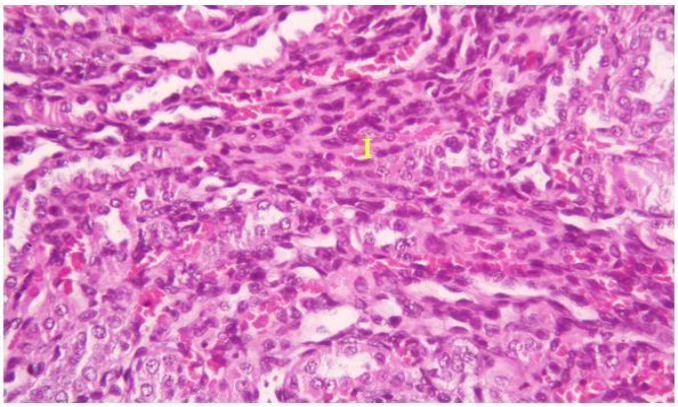

Fig. 15: Photomicrograph of the kidney section of pregnant rat of gr.T3 showing severe infiltration of inflammatory cells (I). (H&E, x400)

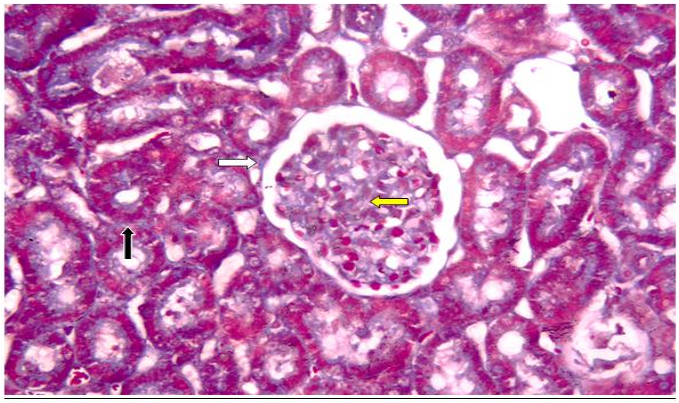

Fig. 16: Photomicrograph of a section of renal cortex of control pregnant rat showing a little collagen fibers in the capsular wall (white arrow), intraglomerular capillaries (yellow arrow) and peritubules (black arrow) (MT, x400)

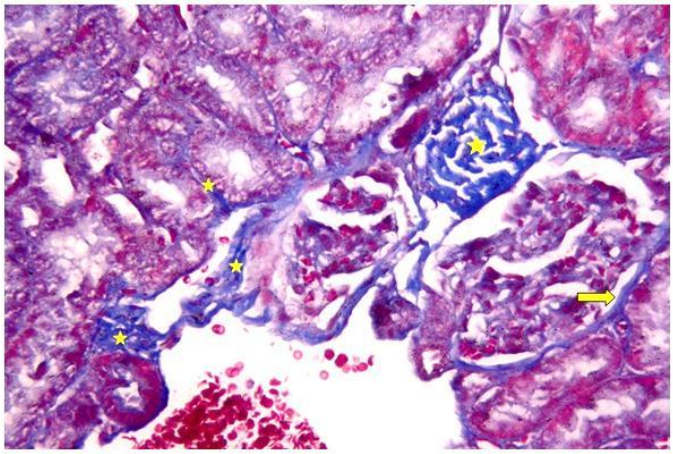

Fig. 17: Photomicrograph of the kidney section of a pregnant rat of gr.T1 showing highly increased collagen fibers confined to the tubular interstitium (asterisk) and pericapsular walls (arrow). (MT, x400)

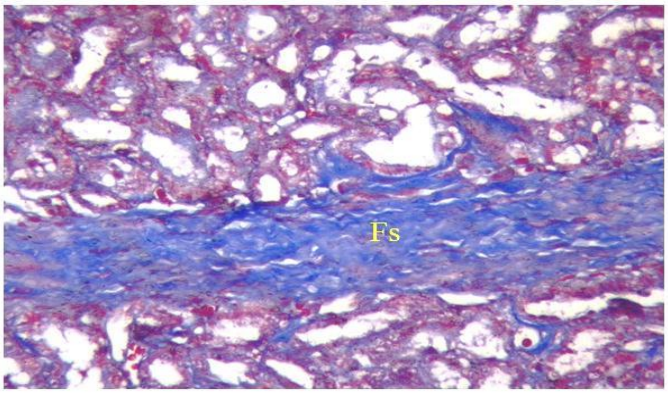

Fig. 18: Photomicrograph of the kidney section of pregnant rat of gr.T1 showing a thick layer of collagen bundles in the interstitium (Fs). (MT, x400)

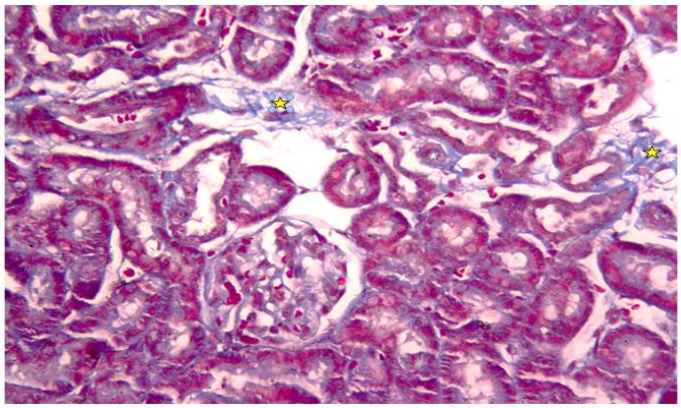

Fig. 19: Photomicrograph of a section of the kidney of a pregnant rat of gr.T2 shows a mild to moderate increased collagen fibres (asterisk). (MT, x400)

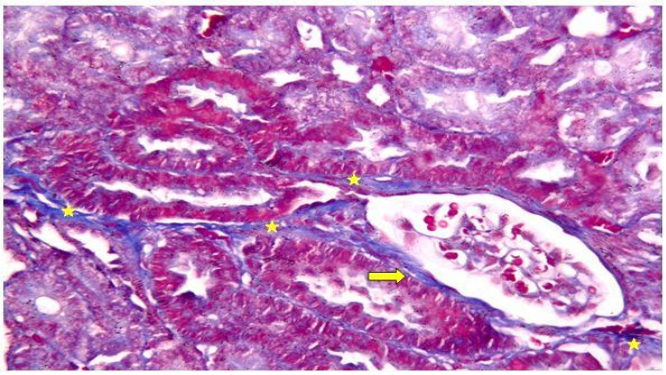

Fig. 20: Photomicrograph of the kidney section of a pregnant rat of gr.T3 showing a lot of collagen fibres around the capsular wall (arrow) and in the basement membrane of the convoluted tubules (asterisk). (MT, x400)

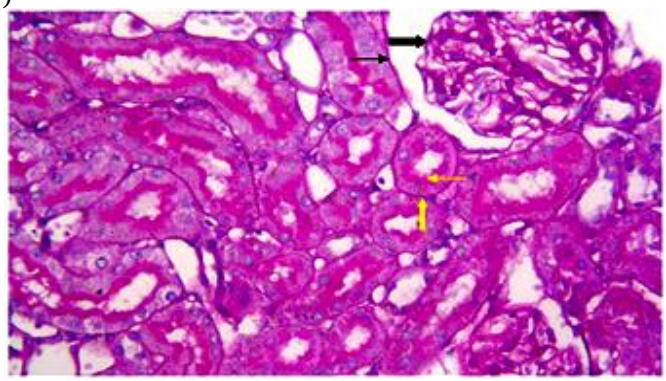

Fig. 21: Photomicrograph of a section of renal cortex of control pregnant rat showing a normal PAS reaction in the glomerulus **(black thick arrow),** Bowman's capsule **(black thin arrow),** the basement membranes of the renal tubules **(yellow thick arrow)** and the brush borders of the proximal convoluted tubules **(yellow thin arrow). (PAS & H, x400)**

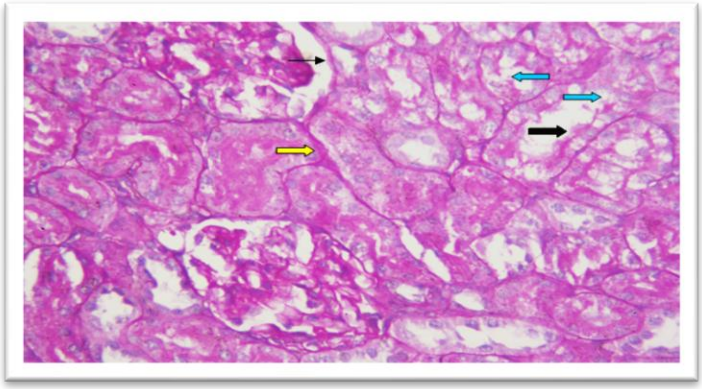

Fig. 22: Photomicrograph of the kidney section of group T1 showing a weak PAS reaction **(black thick arrow)** and destruction in brush borders (**blue arrow)** of some proximal convoluted tubules, also a thickning in the basement membrane of Bowman's capsule **(black thin arrow)** and some renal tubules **(yellow thick arrow)** are shown. **(PAS & H, x400)**

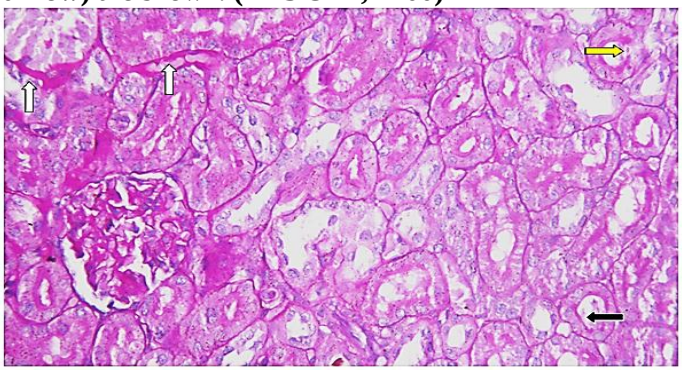

Fig. 23: Photomicrograph of a section of the kidney of group T2 animal showing a weak PAS reaction **(black)** in brush borders **(yellow arrow)** of few PCTs. There is a thickness in the basement membrane **(white arrow)** of some renal tubules.**(PAS & H, x400)**

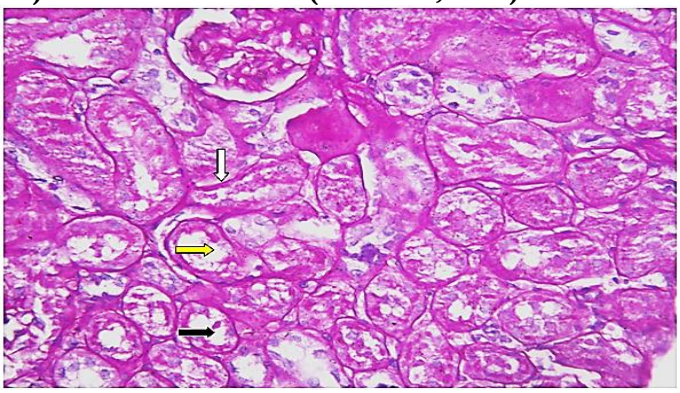

Fig. 24: Photomicrograph of the kidney section of group T3 showing a weak PAS reaction in brush borders **(yellow arrow)** or completely absent brush borders **(black arrow)** of PCTs and a thickness in the tubular basement membranes **(white arrow).(PAS & H, x400)**

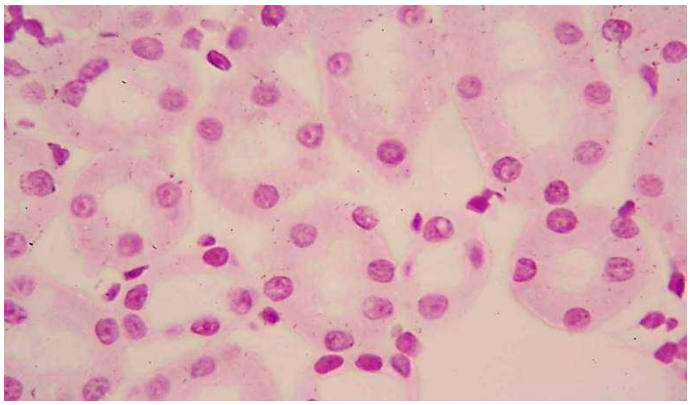

Fig. 25: Light micrograph of a section of renal cortex of control pregnant rat shows a normal distribution of DNA content in the renal tubules. (F, x1000)

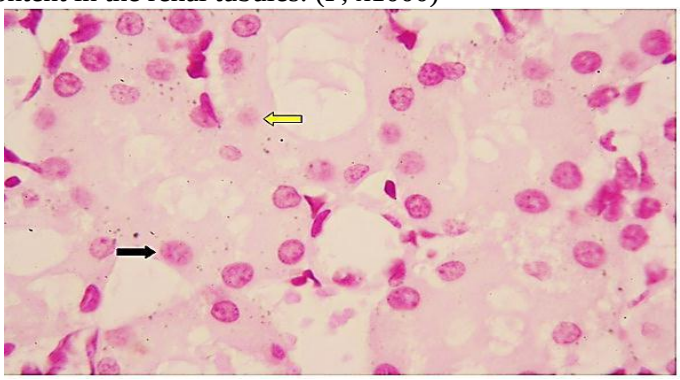

Fig. 26: Light micrograph of the kidney section of group T1 animal showing a decrease in DNA content that appears in the form of faintly stained nuclei in some tubular cells (black arrow). Karyolytic nuclei also appeared (yellow arrow). (F, x1000)

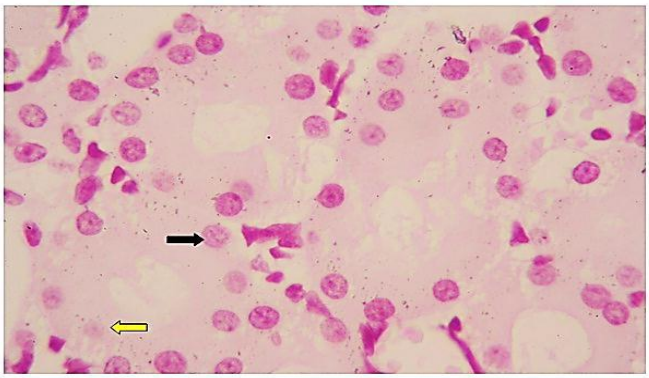

Fig. 27: Light micrograph of a section of the kidney of group T2 animal showing some moderately stained nuclei (black arrow) and other appears in the karyolytic state (yellow arrow)**. (F, x1000)**

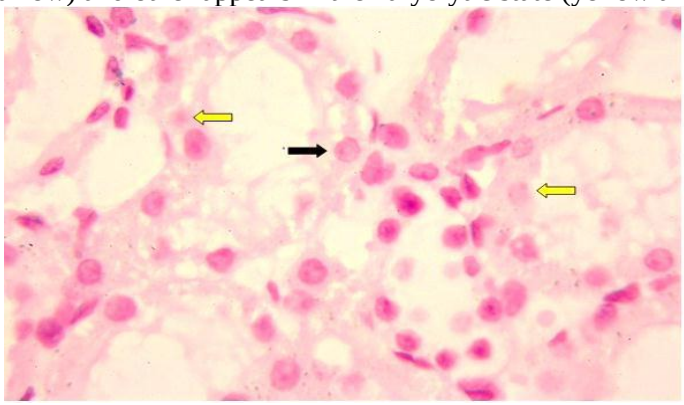

Fig. 28: Light micrograph of the kidney section of group T3 animal showing a weak staining affinity indicating a marked decrease in DNA in the most nuclei of the renal cortex tubules (black arrow) and in the karyolytic nuclei (yellow arrow). (F, x1000)

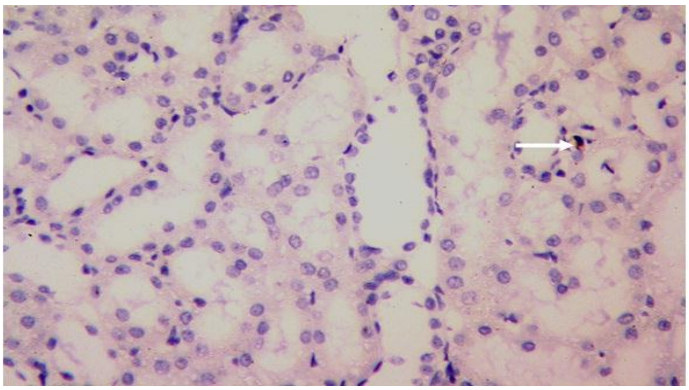

Fig. 29: Light micrograph of a section of kidney cortex of a pregnant rat showing rarely demonstration of CD68-positive reaction for macrophages in the tubular interstitium of control kidney (arrow). (anti.CD68, x400)

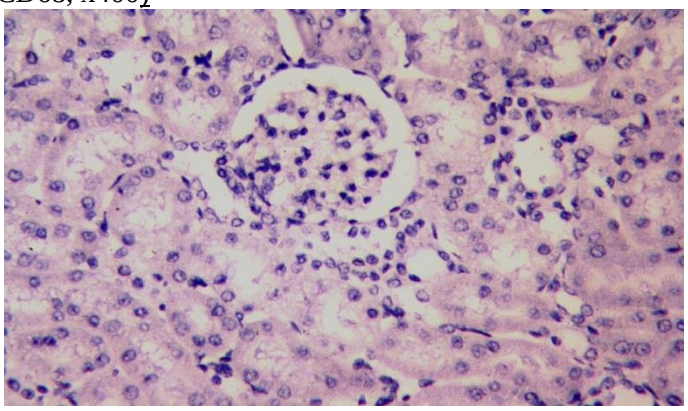

Fig.30: Light micrograph of a section of renal cortex of control pregnant rat showing a negative CD68 immunoreactivity in the cytoplasm of tubular epithelial cells and the mesangial areas. (CD68, x400)

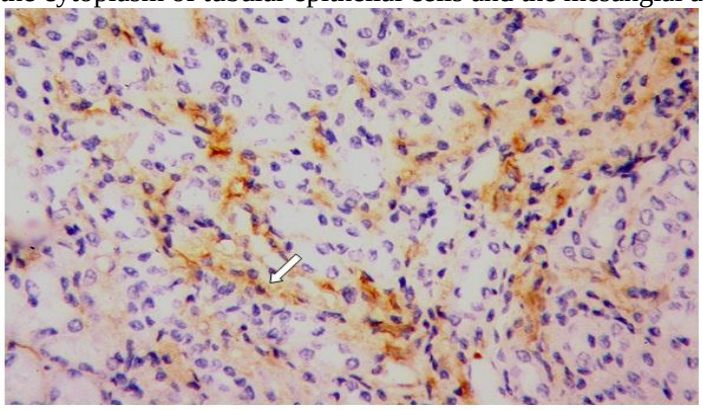

Fig. 31: Light micrograph of the kidney section of pregnant rat of gr.T1showing an intense CD68-positive immunoreaction for macrophage infiltration in the tubulointerstitium (arrow). (CD68, x400)

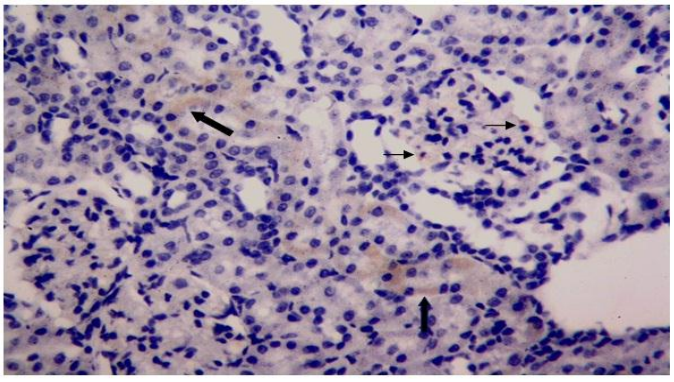

Fig.32: Light micrograph of the cortical kidney section of pregnant rat of gr.T1 rat showing CD68-positive immunoreaction in the cytoplasm of some tubular epithelium (thick arrow) and mild reaction in the mesangial areas (thin arrow).(CD68, x400)

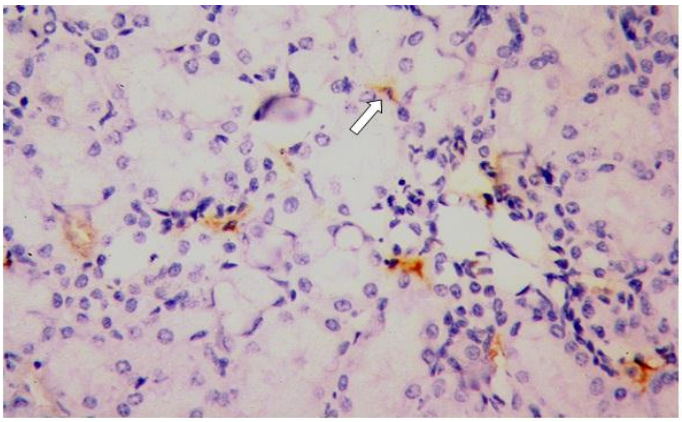

Fig.33: Light micrograph of a section of the kidney of gr.T2 rat showing a moderate CD68-positive reaction in the interstitial areas indicating the presence of few macrophages (arrow).(CD68, x400)

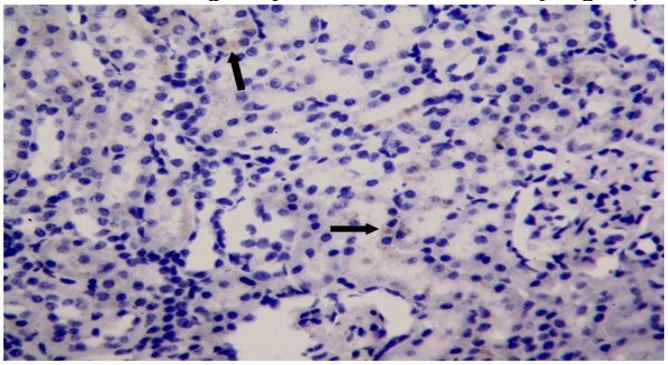

Fig. 34: Light micrograph of a section of the kidney of gr.T2 showing faint CD68-positive reaction in some tubules (arrow). (**CD68, x400)**

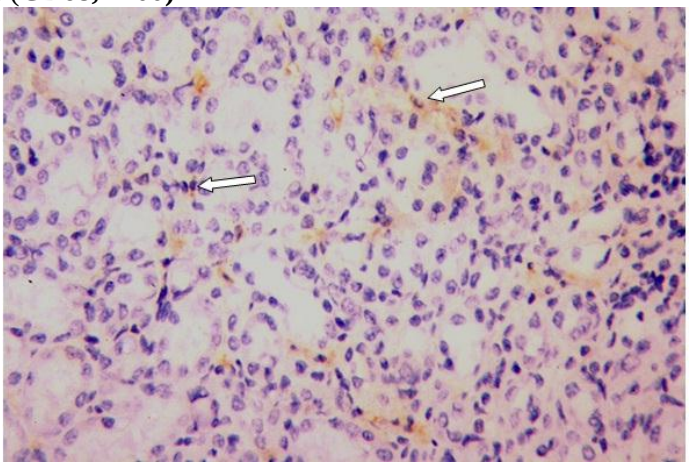

Fig. 35: Light micrograph of the kidney section of animal of gr.T3 showing a high positive immunoreactivity for CD68 in the interstitial tissue (arrow). (CD68, x400)

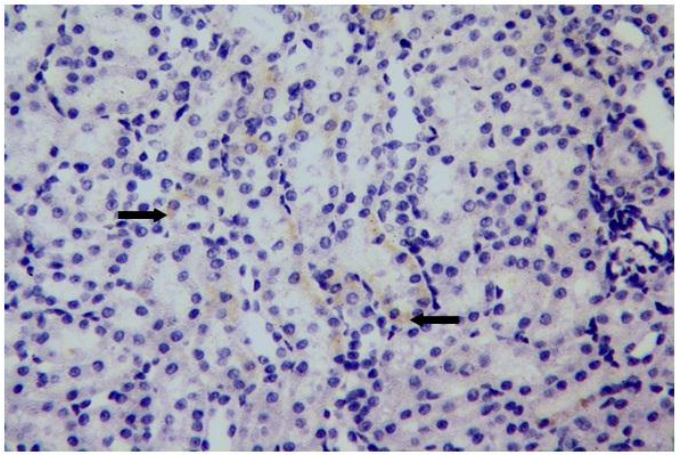

Fig. 36: Light micrograph of the kidney section of animal of grT3 showing a moderate CD68-reaction in some tubules (arrow). (CD68, x400)

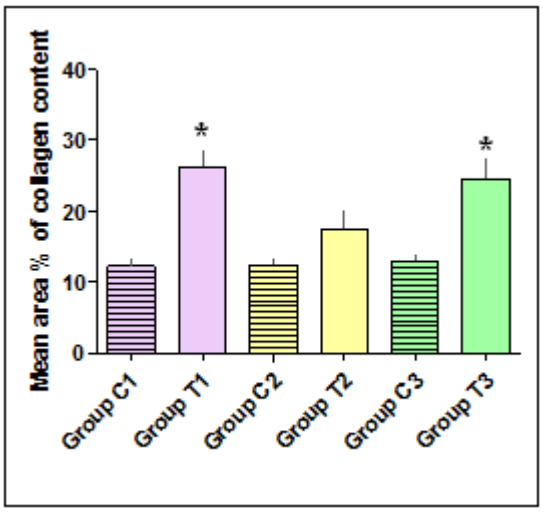

Fig. 37: Histogram showing the mean area % ollagen contents.

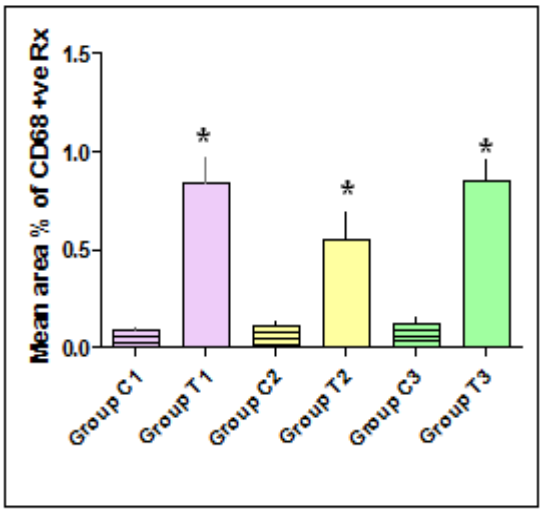

Fig. 38: Histogram showing the mean area % of CD68 +ve Rx.

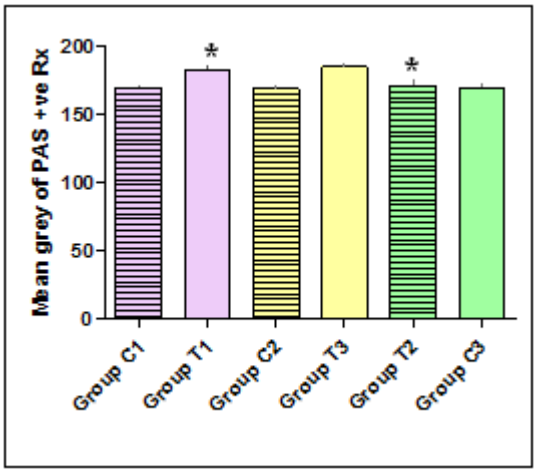

Fig. 39: Histogram showing the mean grey of PAS +ve Rx..

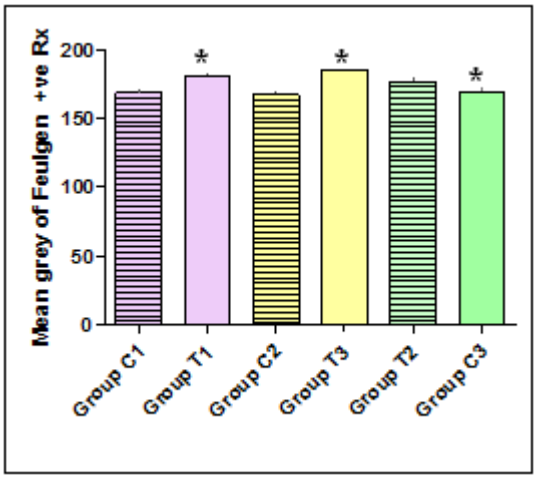

Fig. 40: Histogram showing the mean gray of Feulgen +ve Rx

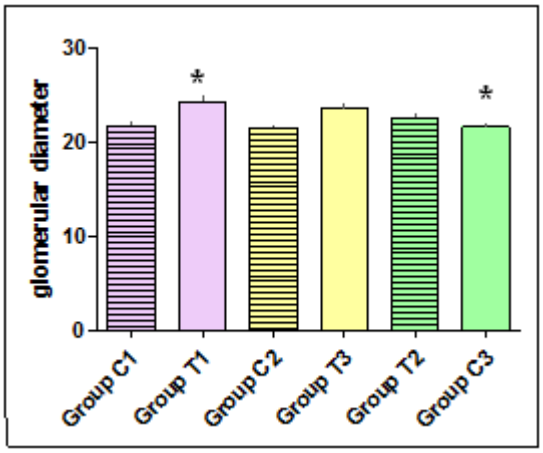

Fig. 41: Histogram showing glomerular diameter of mothers groups.

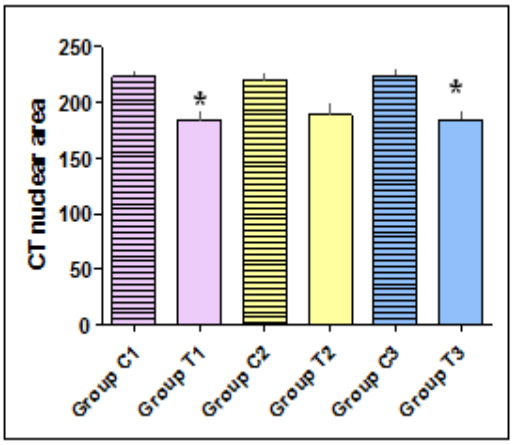

Fig. 42: Histogram showing the convoluted tubules nuclear area of mothers groups.

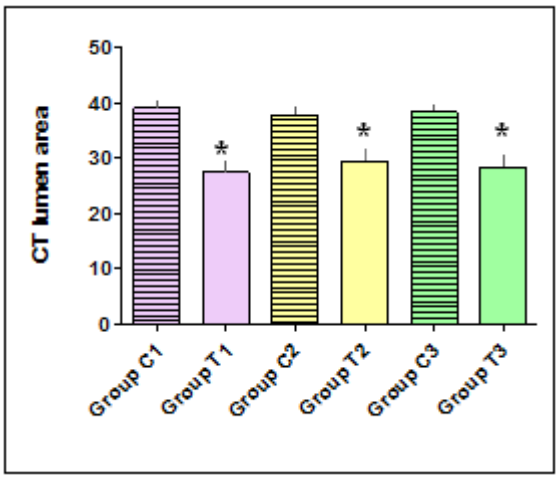

Fig. 43: Histogram showing the convoluted tubules lumen area of mothers groups.

Fig. 44: Histogram showing the convoluted tubules' basement membrane thickness of

.

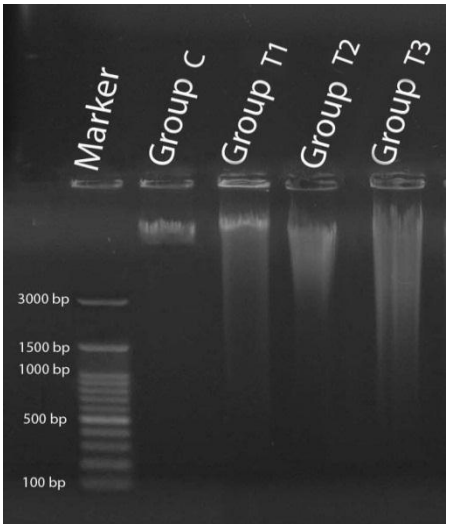

Fig. 45: Agarose gel electrophoresis of genomic DNA isolated from kidneys of pregnant rats mothers groups.

Table (1): Image analysis of mean area % of (collagen contents and the +ve reaction of CD68) and mean grey of (+ve reaction of PAS and Feulgen) of kidneys of pregnant rats.

Parameters / *Groups*	*Collagen Content*	*CD68 +ve Rx*	*PAS +ve Rx*	*Feulgen +ve Rx*
Group C1	12.21±1.134	0.0885±0.02106	169.2±2.754	168.9±2.059
Group T1	26.28±2.390*** (115.23)	0.8390±0.1303*** (848.02)	182.5±2.514* (7.86)	181.0±1.996*** (7.16)
Group C2	12.37±0.706	0.1085±0.02677	168.8±2.152	167.6±1.767
Group T2	17.44±2.586 (41)	0.6269±0.1691* (477.8)	171.1±4.107 (1.36)	177.2±2.683** (5.72)
Group C3	12.89±1.012	0.1255±0.03471	169.4±2.298	169.6±2.010
Group T3	24.61±2.764** (91)	0.8550±0.1113*** (581.3)	185.0±2.542** (9.21)	185.8±0.7862*** (9.55)

The number of animals were 6 in each group.
Data are expressed as mean ± SE.
*****: Significant change at $P < 0.05$ with respect to corresponding control group (C1 or C2 or C3).
( ): % difference with respect to control value

Table (2): Histomorphometrical measurements of the glomerular diameter, and the convoluted tubules (CT) nuclear area, lumen area and basement membrane (BM) thickness in kidneys of mothers rats after clarithromycin administration.

Parameters / *Groups*	*glomerular diameter*	*CT nuclear area*	*CT lumen area*	*CT BM Thickness*
Group C1	21.72±0.3039	223.7±4.591	39.05 ±1.290	2.688±0.08108
Group T1	24.27±0.5976** (11.74)	183.6±8.830** (-17.92)	27.45 ±1.981*** (-29.70)	2.984 ±0.06938 (11.01)
Group C2	21.40±0.3174	219.9±6.130	37.89±1.213	2.661 ±0.08230
Group T2	22.52±0.5195 (5.23)	189.1±9.240* (-14)	29.47 ±2.255** (-22.22)	2.872±0.06846 (7.9)
Group C3	21.57±0.3129	224.5±4.641	38.46±1.142	2.702±0.08461
Group T3	23.54±0.4967* (9.13)	184.1±8.106** (-18)	28.33 ±2.052*** (-26.34)	3.002 ±0.06725 (11.10)

The number of animals were 6 in each group. Data are expressed as mean ± SE.
*****: Significant change at $P < 0.05$ with respect to corresponding control group (C1 or C2 or C3).
( ): % difference with respect to control value.

Table (3): The purity of total genomic DNA isolated from kidney of pregnant rats.

parameters / *Groups*	A_{260}	A_{280}	*DNA Purity* (A_{260}/A_{280})
Group Control	0.15	0.082	1.83
Group T1	0.104	0.057	1.82
Group T2	0.124	0.071	1.75
Group T3	0.131	0.076	1.72